Computer-Aided Civil and Infrastructure Engineering, Volume 31, Issue 9, September 2016, Pages 701–716
DOI:10.1111/mice.12199

A computational methodology for assessing the time-dependent structural performance of electric road infrastructures

Rosario Ceravolo*, Gaetano Miraglia, Cecilia Surace

DISEG (Politecnico di Torino), c. Duca degli Abruzzi 24, 10128 Torino, Italy

&

Luca Zanotti Fragonara

SATM (Cranfield University), College Road, MK43 0AL Cranfield, United Kingdom

Abstract: *An infrastructure adapted to dynamic wireless recharging of electric vehicles is often referred to generically as Electric Road ("e-road"). E-roads are deemed to become essential components of future grid environments and smart city strategies. Several technologies already exist that propose different ways to integrate dynamic inductive charging systems within the infrastructure. One e-road solution uses a very thin rail with box-section made of fibre-reinforced polymer, inside which an electric current flows producing a magnetic field. In spite of the great interest and research generated by recharging technologies, the structural problems of e-roads, including vibrations and structural integrity in the short and/or long period, have received relatively little attention to date. This paper presents a novel computational methodology for assessing the time-dependent structural performance of e-roads, including a recursive strategy for the estimation of the lifetime of surface layers. The paper reports as well some numerical findings about e-roads that will drive further numerical analyses and experimental studies on this novel type of infrastructure. Finally, numerical simulations have been conducted in order to compare an e-road with a traditional road ("t-road"), in terms of static, dynamic and fatigue behaviour.*

1 INTRODUCTION

1.1 Background and motivations

Even though the concept of electro-mobility can be traced back more than 150 years, it is only recently that industry and research centres have started investing in the experimentation of new inductive charging technologies to evaluate their feasibility for real-life operation (e.g. the UNPLUGGED FP7 project, http://unplugged-project.eu/wordpress/, the FABRIC FP7 project, http://www.fabric-project.eu/, the ELECTRIC TEN-T project www.electric-project.eu). Among these, dynamic (en-route) charging would allow vehicles to be recharged while moving without forcing the user to stop (Fisher et al., 2014). Clearly, for a large-scale application of these innovative solutions, different types of problems need to be addressed (Suh, 2011) before being able to optimize the implementation of the charging devices in the urban environment.

To date, very little research has been performed regarding the protection of the charging facilities and road structure against damage due to mechanical loading and the environment (Chen et al., 2015). The same can be said for issues related to vibrations, dynamic amplification at critical points (e.g. viaducts and bridges) and structural integrity in the short and/or long period, which can differ significantly from those of t-roads due to different stress distributions. Therefore, in order to gain some insight into the structural behaviour of the new e-roads, it is necessary to start from the evaluation of criteria and standards related to traditional infrastructures, especially concerning their long-term performances.

A typical problem of traditional infrastructures pertains vibrations induced by traffic, and in fact a large amount of

scientific literature is available on the topic (Ju, 2009; Lak et al., 2011). Vibrations need to monitored and possibly absorbed because of their effects on existing buildings; moreover, today it is increasingly important to evaluate the effects of vibrations on these e-roads implemented with devices potentially compromised by the dynamic interactions (Boys and Covic, 2013a).

A Wireless Power Transmission (WPT) is a system that transmits electric power through the vacuum of space without use wires. In particular, the Inductive Power Transfer (IPT) technology is a typical nearfield WPT technology suited for the contactless charging solution for electric vehicles and e-roads (Chen et al., 2015). In order to optimize the WPT between the e-road and the vehicle, the wear layer of the pavement needs to be very thin. Typical reference values of its thickness are 40-50 mm (Viktoria Swedish ICT, 2013). In such conditions, an excessive dynamic amplification could lead to unexpected damage. In addition, the braking force due to the vehicles could lead to high stress in the wear layer, causing failure of the pavement. In this case, the stress due to a braking force would depend on both the tyre adhesion and the friction between the road layers (Jeong et al., 2014; Perret and Dumont, 2004). Furthermore, the shape and dimensions of the tyre can lead to different effects in the pavement (Dessoukya et al 2014, Hamlata et al, 2014). Nonetheless, for a structural assessment such level of detail is not deemed necessary, since other characteristics as the materials and dimensions of the e-road infrastructure may influence the results much more. Similarly, it is not possible to consider only the surfaces layers of the road in the model. Typical pavement design codes require that the whole pavement structure is modelled in order to consider sublayers or subsurface deformations (Levenberg, 2013). Further considerations apply to jointed concrete pavement solutions consisting of distinct slabs, which are not specifically addressed in this study.

Although the e-road implementation could lead to several issues regarding the short-term behaviour, it is over the long-term that the most significant problems are likely to occur. A key factor in the analysis of the long-term behaviour of the e-road is the material chosen for the asphalt layer because of the influence on its rheological proprieties. A continuum mechanics approach to simulate the asphalt is reported in (Zopf et al., 2015) where the model is subject to a transient cyclic tyre load. Instead, a FE model of flexible pavement with static repeated wheel load is found in (Al-Khateeb et al., 2010). In general, the rutting deformation is known to augment with increasing temperature and tyre pressure and to be inversely proportional with respect to the subgrade strength. Studies that highlight the importance of the rutting phenomenon in the road pavement are reported in (Ahmed and Erlingsson, 2013; Darabi et al., 2012; Qiao et al., 2015; Rahman and Erlingsson, 2015; Saevarsdottir and Erlingsson, 2015). In some e-road solutions, the insertion of charging devices could lead to stress concentration in the proximity of the devices, resulting in an accelerated, deeper rutting.

Rutting is not the sole effect that must be considered in a fatigue analysis. In fact, both cracking evolution and local disintegration are important over the lifetime of the road (Gupta et al., 2014). The methods to evaluate the life of a road pavement are often based on the number of load cycles to failure, the value of which depends on the fatigue model chosen for the analysis. Different approaches exist to evaluate the number of load cycles an asphalt layer underwent, e.g. based on strains, stresses, temperatures or on the dissipated energy (Baburamani, 1999). The most popular models for assessing the fatigue damage accumulated by the pavement are the strain-based ones, which are related to the tensile strain at the bottom of the asphalt layer. More accurate models can be used if the non-linear parameters of the materials are known (Darabi et al., 2012). As previously mentioned, the definition of the number of load cycles to failure is useful to determine the lifetime of an infrastructure or a part of it. However, in order to determine exactly when the infrastructure is in need of maintenance, it is necessary to integrate the phenomenological estimates with an active monitoring procedure that can detect the real damage evolution into the infrastructure. The process of implementing a damage detection and characterization strategy for structures and infrastructures is referred to as Structural Health Monitoring (SHM). This may be done by introducing sensors into the pavement (Čygas et al., 2015) and/or using special techniques such as acoustic emission monitoring (Seo and Kim, 2008). Monitoring is very important because the maintenance and the management of aging civil infrastructure systems, including bridges and tunnels, accounts for 40% of the total construction costs. It has been estimated that the investment needed to enhance the performance of deficient infrastructures exceeds $900 billion worldwide (Fraser et al., 2003). These statistics underline the importance of developing reliable and cost effective techniques for the massive structural rehabilitation and repair investment needed in the years ahead. Without a proper management of the aging civil structures, the failure of these infrastructures could have a major economic impact. Thus, SHM can be integrated with life-cycle management to optimise the maintenance of infrastructure and, possibly, to operate infrastructure systems beyond their original design life (Frangopol and Messervey, 2009; Sarma and Adeli, 2002).

1.2 Structure of the article

In the literature there is a lack of articles dealing with the numerical modelling of new e-roads. From a structural point of view, E-roads mainly differs from t-roads in terms of stress distributions. Consequently, this paper aims to fill the gap, proposing a computational methodology for

investigating the time-dependent structural performance of a typical e-road infrastructure. Based on such a rationale, the results of numerical analyses are presented, with focus on the static, dynamic and fatigue behaviour of the adapted asphalt pavement structure. No further considerations are made in this article on the integrity and life-cycle analysis of charging devices.

Section 2 contains a brief description of existing technologies, together with some pros and cons.

Section 3 describes numerical models for a typical e-road "rail" solution, both for the static and dynamic behaviour. In addition, a comparison between the analysed e-road and a traditional road (t-road) is presented.

The long-term behaviour of the analysed system is presented in Section 4, with the study of visco-elastic and fatigue phenomena that occur in the wear layer of the road pavement. Finally, a recursive strategy is proposed for predicting the lifetime of the e-road subject to standard and heavy vehicles loadings, based on statistical models and FE analyses.

Figure 1 outlines the structure of the article and the general methodology, whose single points will be discussed in detail within each specific section below.

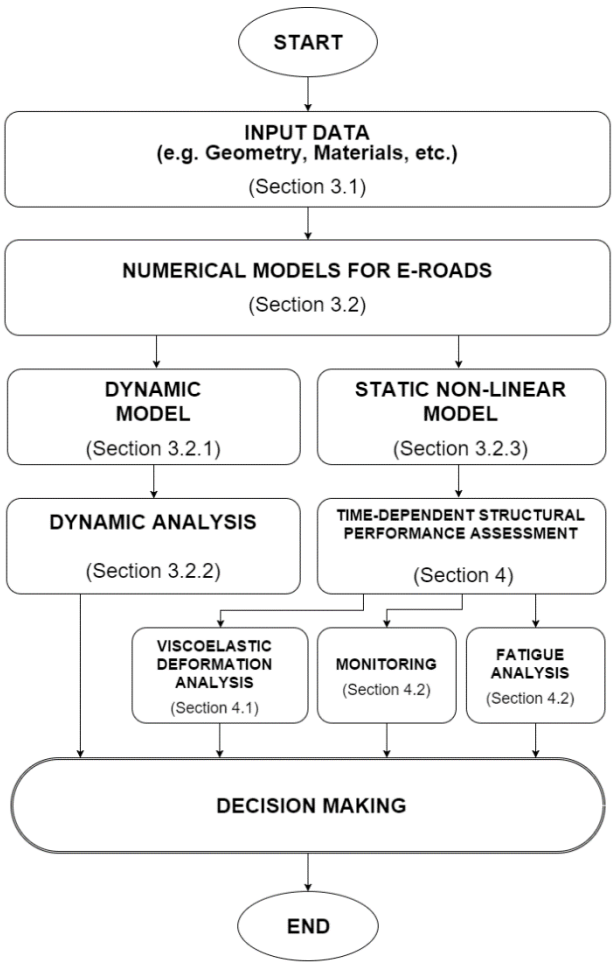

Figure 1 Outline of the article and general methodology.

2 ELECTRIC ROAD SYSTEMS OVERVIEW

The aim of dynamic wireless charging technology is to recharge electric vehicles (EVs) while moving without the need to stop. Being recharged more frequently, the on-board battery would need to have less capacity than a traditional EV's battery (Boys and Covic, 2013b), reducing the weight and the price of EVs. In addition, it is known that lower depth of discharging extends the life span of batteries (Guena and Leblanc, 2006). Another long-term advantage could be to exploit EVs as mobile energy storage systems, allowing surplus of electrical energy to be stored during the hours of low consumptions and be released when energy demand is higher, thus reducing CO_2 emissions. However, the infrastructure could be very expensive to implement (Gill et al., 2014).

Several innovative technology providers are currently working to develop inductive static and/or dynamic wireless charging technologies for electric vehicles and a variety of other applications. In particular, a certain number of patents exist that propose different ways to integrate the

dynamic inductive charging systems with the infrastructure, even though the solutions that are deemed suitable for real applications are in very limited number.

As for other innovative technologies, e-roads should ensure an adequate health and safety's level, i.e. a low electromagnetic field (EMF) exposure. The EMF effects depend on the exposure time, the operational frequency and the EMF level reached during the power transfer. In addition, the EMF could interfere with pacemakers or other life-support devices. For these reasons, the International Commission on Non-Ionizing Radiation Protection (ICNIRP) is developing a series of guidelines for the maximum levels of EMF achievable during the power transfer (ICNIRP, 1998; ICNIRP, 2010).

In addition to the health and safety issues, a very important aspect to consider is the cost related to the new e-roads. As far as the electrification cost of the infrastructure is concerned, some reference values may be found in (Gill et al., 2014) and (Schroeder and Traber, 2012). In 1990, UC Berkeley conducted one of the most complete studies about the costs arising from the realization of an e-road, estimating a cost of 1,000,000 $/km per road lane. For new installations, "electrification" has been estimated to add less than 10% to the cost of a traditional infrastructure.

For an actual feasibility, the new e-roads should reach high efficiencies in terms of power transferred, air-gap allowed between the two coils, transverse misalignments and efficiency of the power transfer (Suh, 2011; Covic and Boys, 2013).

The Korean Advanced Institute of Science and Technology (KAIST) has already developed different solutions for WPT that can be summarised in 5 generations (Rim, 2013). In 2009, the first technology generation for golf carts was presented. The same year, were presented two more technologies: one, also called mono-type technology, was applied to buses but achieved poor results. The third generation (3G) technology used an innovative Shaped Magnetic Field In Resonance (SMFIR) technology that improved considerably the system's efficiency (Boys and Covic, 2013b) by decreasing the width of power rail from 1.4 m to 0.8 m.

For the 4th generation (4G), the Department of Nuclear and Quantum Engineering of KAIST developed a new wireless charging device suitable for modular and large-scale production, significantly reducing the cost for the implementation of the e-road (olev.kaist.ac.kr, 2012).

The 4G system consists of a rail inserted in the pavement without using a cover layer. An inverter separates each rail defining several sub-rails (the real charging-units). For the 4G technology were proposed three rail segmentations for this generation, each with different advantages and disadvantages (Rim, 2013).

In order to optimize the magnetic field *B* shape, some "I"-shaped ferrite cores (a fragile ceramic magnetic material) aligned with the motion direction are positioned in the box-section, with several electric cables coiled around them. The rail is approximately 0.1 m wide (about 1/8 of the width of the previous generation) and 0.3 m deep. With this new solution, the power transferred increases up to 25 kW, enough to recharge a bus. Furthermore, the misalignment permitted during the motion reaches 24 cm, with a value of magnetic field less than 1 μT (in compliance with international guidelines) and with an air-gap of 20 cm. Finally, comparing with the previous generations, the new technology needs only 1/10 of the time for construction and 80% of the cost (Rim, 2013).

Today the 5th generation (5G) is under development. It is expected to be similar to the 4G one but the charging-unit should be narrower and it should contain a ferrite core with a more efficient S-shape for WPT (Rim and Lixin, electricvehicle.ieee.org, 2014).

The 4G rail technology (and consequently 5G) should be significantly less invasive than the existing ones, affecting just a strip 0.1 m wide in the lane. Implementation should be relatively easy and fast and, since there are no coatings, should also be ideal for maintenance operation. However, without a surface layer, the power rail would be subject to strong mechanical, physical and chemical actions that, if not properly catered for, could lead to a shorter lifetime of charging-unit. In addition, the unit may be affected by the environmental conditions which, during the life span of infrastructure, could vary from -40 °C to +65 °C, depending on the climate. For this reason, for the design the charging-unit, highly versatile materials, such as polyurethane, ABS (Acrylonitrile-Butadiene-Styrene), resins etc. should be used (Boys and Covic, 2013b). For the coil-box, polymer materials (or their blends) should be chosen to not interfere with electromagnetic field produced for the WPT (Boys and Covic, 2013b). In addition, for what concerns the stiffness of the materials used in the infrastructures, polymers could be a good choice to implement the e-roads, especially as regards long-term behaviour of the surface layers.

3 NUMERICAL ANALYSES

Modelling constitutes the first research gap that needs to be addressed in order to optimize the benefits of the e-roads across a wide range of users and applications.

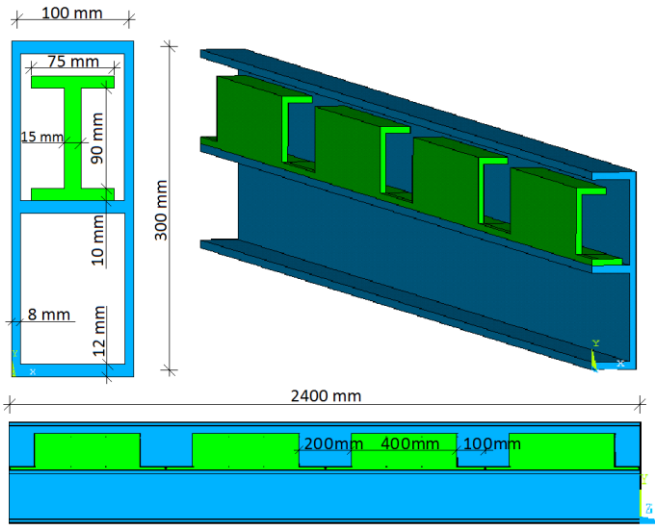

Figure 2 Modelled recharging unit.

Table 1
Material elastic properties: Young modulus, E, Poisson's coefficient, ν, density, ρ (Park et al., 2005; www.icpdas.com/faq/Cycoloybrochure.pdf; www.ferrite-info.com/characteristics.aspx).

Mat. ID	*Structural Element*	E [MPa]	ν	ρ [kg/m^3]
1	Surface layer	6,500	0.3	2,500
2	Base layer	130	0.35	2,200
3	Sub-base layer	90	0.4	1,200
4	Polymer coil-box	2,200	0.35	1,150
5	Sub-grade layer	3,000	0.4	2,000
6	Ferrite core	180,000	0.28	5,000

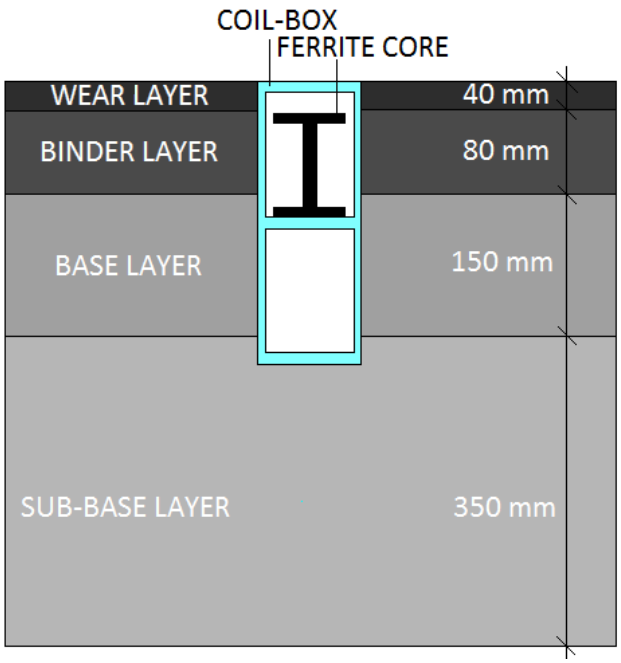

Figure 3 E-road pavement structure with layers and the charging unit installed in the middle of road lane.

3.1 Materials and geometry of a typical "rail" solution

The thickness of the vertical panels of the rails is of 0.8 cm, while the horizontal ones are 1.2 cm thick. In the upper box (see Figure 2), there is an I-shaped ferrite core with flange dimension of about 1x7.5 cm and the web of 1.5x9 cm. The ferrite core is composed by 4 sub-cores, as Figure 2 shows. Each sub-core has a bottom flange 60 cm long connected with the adjacent ones.

The vertical wall and the upper wing length is 40 cm and are 20 cm spaced from the adjacent components. The total length of the charging-unit is 2.4 m, which is inserted in the road pavement at the middle of a road lane. Other details can be found in Rim et al. (2013).

In this study, the assembly e-road is modelled as 3 layers structure on elastic springs, not differently from a t-road except for the recharging unit. The surface layer is 0.12 m deep, with which both wear and binder layers were described. The base course layer is 0.15 m deep, while the sub-base layer is 0.35 m deep (Park et al., 2005). Finally, the sub-grade layer is represented by Winkler soil springs. Table 1 reports the characteristics of the modelled materials. For all materials, a linear elastic behaviour was assumed, this being a common simplification in the literature about short-term pavement analysis (Beskou and Theodorakopoulos, 2011). The structure of the modelled pavement is reported in Figure 3.

3.2 FE models for e-roads

FE models can be successfully used to simulate road and pavement problems that could not be modelled using simpler multi-layer elastic theories. This is particularly true in the case of e-roads, which are characterised by the presence of several charging components that affect the geometry of the road structure. The creation of a linear FE model represents the first step towards the structural assessment of e-roads.

Due to the irregularities of geometry, in the ANSYS® environment, the e-road was modelled with elements representing high stress gradients (near the interface coil-box/pavement) and able to adapt to non-simple geometries (e.g. circular sides, inner corners to the model etc.). Moreover, given the interest for extending investigations to local effects, the chosen elements should support adaptation to various mesh densities. Elements that meet all these requisites are, for instance, 3D hexahedral 20 nodes or 2D rectangular 8 nodes. Moreover, contact elements can be used to simulate the interaction between the charging-unit and the pavement.

Accordingly to the results of a sensitivity analysis, the extension of the models in the horizontal (transverse) direction was set to 3 m. For 3d model, in longitudinal (travel) direction the charging-unit is fully restrained to the switch-boxes, thus the extension of FE model in this direction was fixed to 2.4 m. The FE element size was defined accordingly to a parametric study on the error in strain energy estimation conducted under static loads. Consequently, the ratio between element size and layer thickness was set at 3, apart from the region near the charging unit where a more refined discretization was used. Such discretization allows to capture the wavelengths corresponding to all significant modes in the range 0-90 Hz.

In dynamics, damping characteristics must be defined. The road infrastructure is a heterogeneous structure composed of materials with different behaviours in both static and dynamics. In particular, the infrastructure is formed by several geo-materials, which mechanical proprieties (e.g. damping ratio) are strongly influenced by the strain levels achieved during the load application (D'Elia et al., 2003) (changes up to 20%) and which vary according to the degree of consolidation and type of material (clay, sand, gravel, rock, etc.). Under equal conditions (degree of consolidation, plasticity index etc.) and for the same material type, the damping ratio has a similar trend as a function of strain. From the analyses performed, strains resulted to be of about 10-100 μ-strain. For such values, the damping ratio ζ can be set between 0.5% and 4-5%, while the apparent shear modulus G decreases up to 10% of the elastic modulus G_0, because of the non-linear behaviour of geo-materials, as shown in Figure . In order to study the response of the e-road to harmonic loading, the average value of damping ratio (ζ =2.5%) was assigned to all vibration modes. For transient analysis, instead of one single value of damping ratio assigned to the entire structure, a Rayleigh's damping form was assumed using only one Rayleigh's parameter with which the damping matrix of structure is determined. As a result, damping equal to 2.5% on the predominant frequency was assumed in accordance with data from literature (Zhang et al., 2005).

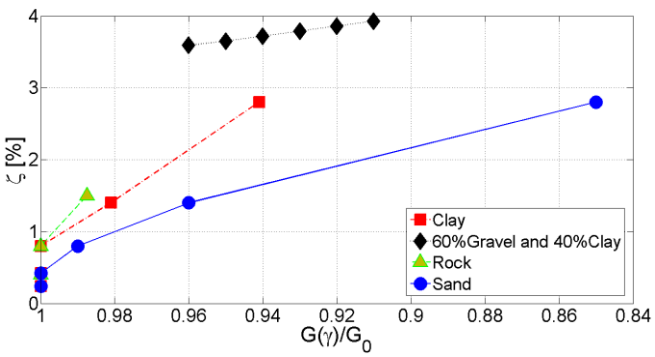

Figure 4 Damping ratio for sundry geo-materials (D'Elia et al., 2003).

3.2.1 Dynamic model

The first four modal frequencies computed using the FE model of the e-road are reported in Table 2. For the sake of brevity, only the first and third modal shapes are shown in Figure , since they lead to the highest modal displacements in the middle of the charging-unit. The vibrations induced by vehicles on the infrastructure are a consequence of the roughness of the road surface and the interaction with the vehicle. The excitation spectrum depends from the vehicle speed and the asperity profile. Common excitations range from 1 Hz to 50 Hz, with higher concentration around 10 Hz (Agostinacchio et al., 2013).

Table 2
Numerical frequencies predicted by 2D FE model.

Mode	*E-Road Frequency* [Hz]	*T-Road Frequency* [Hz]
1	35.1	34.8
2	41.1	41.6
3	60.4	60.2
4	73.3	88.7

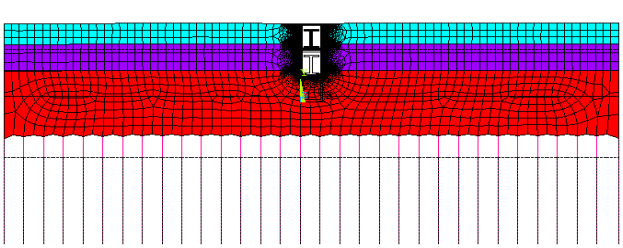

(a)

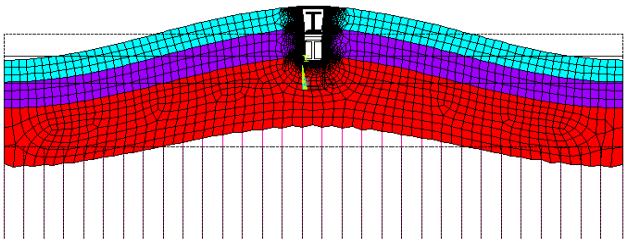

(b)

Figure 5 First (a) and third (b) vibration modes predicted by the 2D FE model of the e-road pavement (charging unit installed in the middle of road lane). The vertical lines along y direction (axis identified by a yellow triangle in the figure) represents Winkler springs.

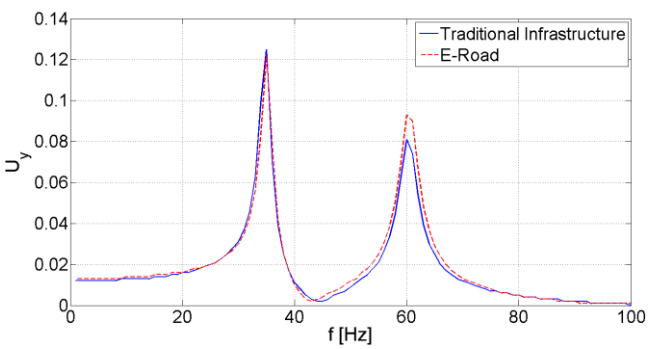

(a)

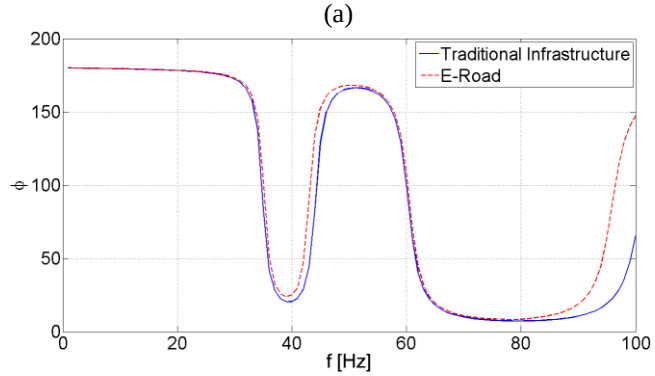

(b)

Figure 6 FRFs for the e-road and for the t-road, calculated with respect to the vertical displacement U_y, at point *D* (see Figure 10). Amplitude (a) and Phase (b).

Figure 6 shows the comparison of the Frequency Response Functions (FRFs) of the t-road and e-road of the response measured in point *D* (see Figure 10) with respect to a vertical excitation applied in the middle of the surface layer. For both the traditional and the electric road, the same damping value, ζ=2.5% (Zhang et al, 2005), was assumed for all modes, due to the unavailability of experimental data. From a linear analysis in terms of FRFs, no appreciable differences in the dynamic response of the two road solutions came to light. Experimental testing will be needed in the near future to detect possible changes in the dissipation properties induced by the e-road adaptation.

3.2.2 Dynamic response of the e-road

In order to evaluate the dynamic behaviour of the e-road, a 3D transient analysis was performed. The passage of a heavy vehicle was simulated in the model with a time-history of the force acting on the pavement, the aim being to compare numerical results with experimental data taken from the literature. The dynamic loading on the pavement was calculated through an algorithm, developed in MATLAB environment (Pinotti, 2013), which supplies the reactions transmitted by a 7-DOF vehicle system subjected to the surface roughness of the asphalt, the inertia forces and the electromagnetic actions of the coils. The 7-dof vehicle model is reported in Figure 7.

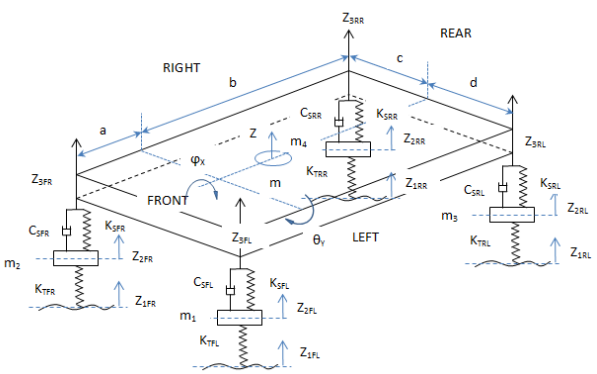

Figure 7 7-dof vehicle model (Syabillah, 2012).

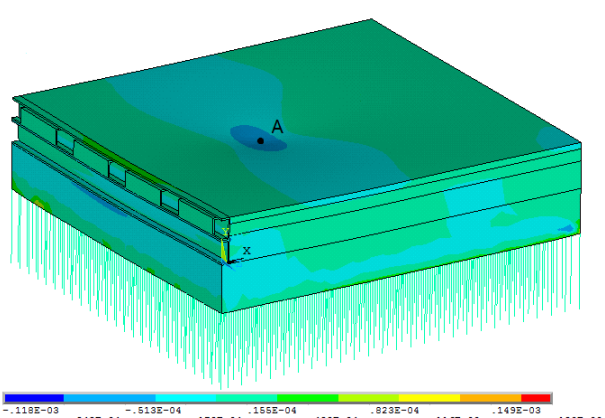

Figure 8 Horizontal transverse strain ε_x distribution at t=0.225 s.

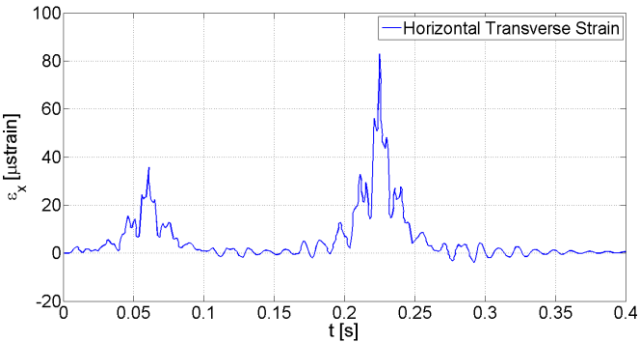

Figure 9 Horizontal transverse strain ε_x [μstrain] evaluated at the point of maximum deflection *A* (see figure 8) and at 0.04 m from the road surface.

The four forces acting on the road due to the interaction between the tyre and surface asperities of the pavement are calculated for a given vehicle speed in the assumption of a rigid flooring. The total output forces are then applied in the FE model as a moving impulse load. It is worth noticing that in some specific cases (e.g. bridges or lightweigth section of the support) it would be necessary to consider the coupled problem.

Figure depicts the horizontal transverse strain ε_x distribution induced in the pavement by the passage of the electric vehicle at 70 km/h. The point of application of the force, *A*, is placed at x=1 m from the centre of the charging device, simulating in this way the vehicle's width. Due to the symmetry of the loads and geometry, only half of the road is represented. Figure 9 reports the time-history of the horizontal transversal strain ε_x calculated in *A*, whose values for the e-road are thus estimated in the range of about 30-80 μstrain. Considering the linearity of the model and the actual range values detected for a traditional infrastructure from 10 to 250 μstrain (also influenced by the temperature) (Čygas et al., 2015), the introduction of a rail charging system is not expected to change appreciably the levels of stress and strain in an existing infrastructure, far from the WPT technology. In any case, the stress and strain distribution in the pavement near the charging device requires more investigations.

3.2.3 Stress/strain distribution in the e-road and non-linear effects

In order to investigate the stress and strain distribution, the 2D FE models were loaded with a pressure load of 1 MPa centred over the rail technology, with a square footprint of 0.3 m.

Figure 11 shows the horizontal normal stress σ_x in the e-road when the coil-box and road pavement are considered bonded. This simplified case (without joints) even if not fully realistic, provides useful results to be compared with the ones of the model using contact elements.

In addition, a more refined FE model with contact elements between the coil and the pavement layers has been developed. The type of contact used is a "standard contact" that takes into account both the friction and the separation behaviour (Metrisin, 2008). One of the most important contact parameters, the normal penalty stiffness factor, was set at 0.3 after several trials (thin box section).

As for the values of σ_x, three representative points were considered in order to compare the stress predicted by the two models with and without the contact elements. In point *B* (see Figure 10), which is characterised by a negative stress (compression), the difference between $\sigma_{x.nc}$ (value calculated without taking into account the contact behaviour) and $\sigma_{x.c}$ (calculated taking into account the contact) is negligible: -3.3 MPa for $\sigma_{x.nc}$ compared to -2.9 MPa for $\sigma_{x.c}$. The same considerations cannot be done for the point *C*, where the stress value supplied by the two models differs more than 10 times: 3.1 MPa for $\sigma_{x.nc}$ compared to 0.2 MPa for $\sigma_{x.c}$. This is essentially due to the presence of the contact elements, which tend to isolate the charging system from the surrounding pavement, not taking into account tensile stresses between the two structures.

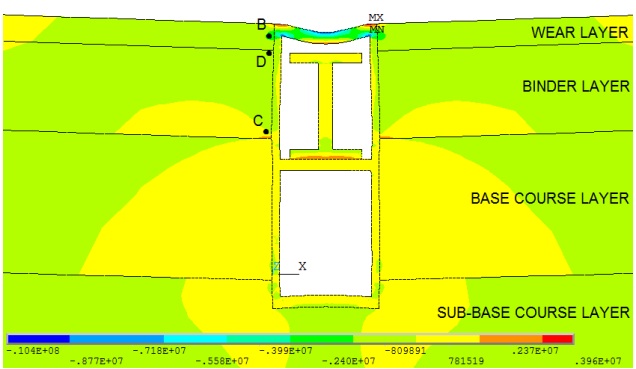

Figure 10 Horizontal transverse stress σ_x [Pa] in the models without contact elements.

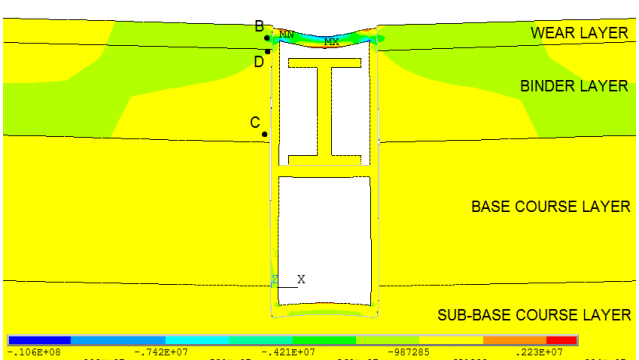

Figure 11 Horizontal transverse stress σ_x [Pa] in the model with contact elements.

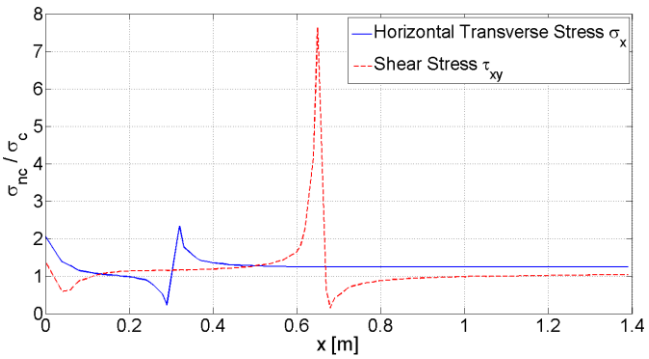

Figure 12 Stress ratio between the values predicted without and with contact elements at the bottom of the wear layer, from the point *D* to the edge of road in horizontal transverse x direction.

Figure 2 shows σ_x and τ_{xy} in terms of the ratio of their values predicted by the no-contact and the contact model at the bottom of the wear layer, along the direction perpendicular to the traveling one.

On account of the observed difference in the stress distribution between the models with and without contact elements (see Figure 10 and Figure 1), the e-road is expected to behave differently from a traditional infrastructure. In fact, models with contact are able to represent the peculiarity of e-roads represented by the unilateral interaction between the pavement and the charging device adaptation.

Figure 3 and Figure 4 show the normal and shear stresses (σ_x and τ_{xy}), respectively, at the bottom of the wear layer along the transverse direction of road. These diagrams compare the e-road and t-road solutions: σ_x may easily differ of about the 100%, with the traditional infrastructure being penalised for x less than 0.3 m. At greater distances from the charging device, where the stress is positive, the difference between the two solutions becomes negligible. The shear stresses τ_{xy} are typically higher for the traditional road, as shown in Figure .

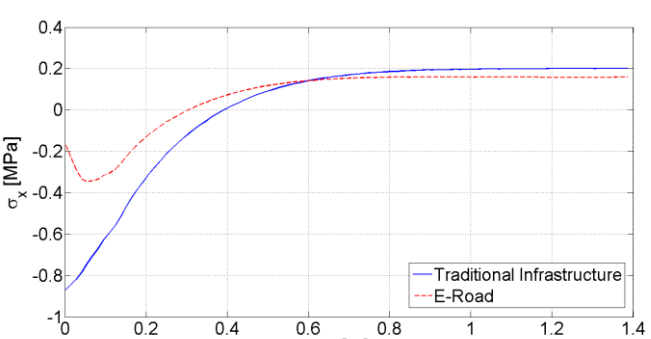

Figure 13 Horizontal normal stress σ_x [MPa] at 0.04 m from the road surface, from the point *D* to the edge of road in horizontal transverse *x* direction.

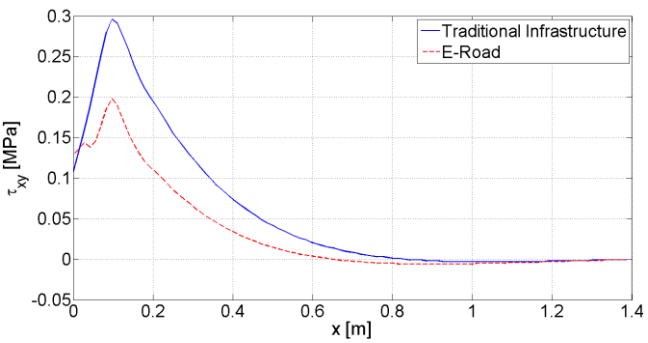

Figure 14 Shear stress τ_{xy} [MPa] at 0.04 m from the road surface, from the point *D* to the edge of road in horizontal transverse *x* direction.

Indeed, the difference in the stress distribution predicted for the e-road and for a traditional infrastructure can vary considerably depending on the depth where the distribution is evaluated. This highlights the importance of using, and possibly refining, contact models at the interface between the charging technology elements and the infrastructure layers, in order to better estimate the real behaviour of the e-road. On the other hand, the introduction of contact elements may lead to several numerical issues that should be bypassed.

Generally, these elements can have linear or non-linear behaviour, while, for the analysed problem, the presence of friction between the coil-box and pavement, and the unbounded characteristic of the contact, results in a non-linear behaviour. For that reason, all the advantages of linear analysis would be virtually lost, especially when it comes to the dynamic characterization of the infrastructure, or to the evaluation of the cyclic loads effects in the pavement such as rutting phenomenon. Therefore, as a first approximation, the dynamic amplification factors has been evaluated by neglecting the contact effects. Future works will be needed to verify this assumption.

4 ASSESSMENT OF THE TIME-DEPENDENT STRUCTURAL PERFORMANCE OF E-ROADS

In order to evaluate the long-term performance of an infrastructure, it is necessary to assess the effects that various actions may determine with respect to the technology and the surrounding environment. The actions can be broadly classified into physical, such as thermal cycling, chemical and mechanical, such as vehicle load.

The long-term behaviour of road pavements, such as the evaluation of the visco-deformation and fatigue, has been the object of a considerable amount of research. The generalized viscoelastic Maxwell model is commonly assumed for asphalt materials, even though visco-elasto-plastic models are also available for road materials (Lu et al, 2014). In this context, there are two principal types of approaches for the evaluation of the rutting depth in the

pavement: (i) dynamic cyclic analysis; (ii) equivalent load approaches. Although the first approach is certainly the most realistic one since vehicles transmit dynamic actions, its use is limited to a small number of cycles due to its high computational demand. The equivalent load approach, instead, consists in defining the time of application of an equivalent load as the product between the single load duration and the number of load cycles (Kettil et al., 2007).

Besides the asphalt itself, also the behaviour of geo-materials needs to be modelled appropriately. For instance, grey-box models and their derivations can be used to predict permanent deformations under cyclic loads. Such models are developed starting from a great amount of experimental data on the materials underlying the wear and binder layers of the road structure (Ren et al., 2012).

In addition to the evaluation of the time dependent deformation in road pavement layers, the number of load cycles to failure should be properly estimated. As stated in the introduction, this can be achieved through a number of empirical methods, some of which imply the use of phenomenological laws for the asphalt layer of pavement. Such laws correlate the number of load cycles to failure, N_f , to the value of tensile transverse strain at the bottom of the surface layer of pavement (Pais et al., 2009; Ren et al., 2012; Zhou et al., 2007).

As for the vehicle load and its distribution, it must be considered that heavy vehicles are responsible of a high percentage of damage. Accordingly, the computational methodology proposed for the structural assessment of e-roads is founded on the following points.

i) A bimodal statistical distribution of the load intensity q is adopted in order to account for heavy vehicles:

$$\hat{B}(q) = p_s \cdot \phi_s(q, \mu_s, \sigma_s) + p_w \cdot \phi_w(q, \mu_w, \sigma_w) \qquad (1)$$

where p_w is the probability of passage of a heavy vehicle and p_s is its complement to one, (1-p_w); $\phi_s(\mu_s, \sigma_s)$ and $\phi_w(\mu_w, \sigma_w)$ are the normal cumulative distribution functions (average, μ, and variance, σ) for standard and heavy vehicles, respectively.

ii) For the number of arriving vehicles, standard and heavy ones, n_s and n_w, a thinned Poisson process is assumed. The inter-arrival time is calculated accordingly.

iii) Based on the two points stated above, the probabilities, Q_s and Q_w, are calculated for the vehicle load not exceed a generic q value in the reference period, t_f. In the two cases of normal and heavy vehicles, the cumulative distributions will be:

$$Q_s(q) = e^{-\lambda\, p_s t_f [1-\phi_s(q)]} \qquad (3.a)$$

$$Q_w(q) = e^{-\lambda\, p_w t_f [1-\phi_w(q)]} \qquad (3.b)$$

where $\lambda\, p_s$ and $\lambda\, p_w$ are the average arrival rates.

The axle load is evaluated by dividing the percentile values, q_{95s} and q_{95w}, by the number of axles, a_s and a_w, corresponding to standard and heavy vehicles respectively, and similarly for the axle inter-arrival times, T_{95as} and T_{95aw}.

iv) Both Gaussian and Laplace distributions (Blab and Litzka, 1995; Harris, 2007) are considered to redistribute T_{95as} and T_{95aw} in the transverse direction of the road lane, x, so as to obtain $T_{95as}(x)$ and $T_{95aw}(x)$, respectively.

Diagrams of the time-dependent structural performance of e-roads have been produced both for recorded data taken from literature and for Highway Capacity Manual (HCM) (National Research Council, 2000) design loads. To this aim a generalised visco-elastic Maxwell law and a deterministic fatigue model were used.

4.1 Viscoelastic deformations

In this paper, in order to simulate the cyclic effect of the vehicle load, the values of viscosity for materials (e.g. bituminous conglomerate) were modified so as to account for the inter-arrival time and for the time duration of the load transmitted over the road section. In more detail, a constitutive viscoelastic Maxwell law is adopted as reference to modify the viscosity value of asphalt layers. Then, an equivalent viscosity is introduced in the generalised Maxwell model. The equivalent viscosity represents the viscosity that in a static analysis would provide the same visco-strain that would be obtained with a cyclic analysis. Accordingly, this parameter is defined as:

$$\eta_{eq}(x) = \eta \frac{T_a(x)}{\tau_a} \qquad (4)$$

where:

- η, is the viscosity of asphalt layers;
- $T_a(x)$, is the inter-arrival time, i.e. the probabilistic period of time which elapses between vehicle axles passing successively on a path of a road section;
- τ_a, is the time duration of the single load cycle, estimated as the ratio between the size of the footprint area (in the direction of travel) and the vehicle speed.

Based on the assumed model, the evolution of the long-term visco-deformation in a Maxwell model will assume the following linear trend:

$$\varepsilon_{v,eq}(x,t) = \frac{\sigma(x)}{\eta_{eq}(x)} t \qquad (5)$$

where $\sigma(x)$ is the stress at the generic transverse position where the equivalent visco-strain is evaluated.

Clearly, working in terms of equivalent viscosity is analogous to defining the time duration of an equivalent static load, which would correspond to the classical

approach, with t/T_a representing the number of load cycles at time *t*.

The importance of the equivalent viscosity approach is not only represented by the advantage of performing long-term assessments with small computational time, but also in the fact that the non-linear contact elements, used in the e-road model to connect the charging-devices to the road pavement, would make it difficult to perform a full dynamic analysis.

The non-linearity to be accounted in the e-road model is due to the interaction between the two surfaces in contact, which implies a recursive search of the normal contact force F_n and the stress exchanged between the same surfaces. The standard procedure employed for the solution is based on the Augmented Lagrangian method (Adeli and Cheng, 1994):

$$F_n = \begin{cases} 0, & g > 0 \\ k_n g + \lambda_n^{i+1}, & g \leq 0 \end{cases} \quad (6.a)$$

$$\lambda_n^{i+1} = \begin{cases} \lambda_n^i + \alpha k_n g, & |g| \geq g_t \\ \lambda_n^i, & |g| < g_t \end{cases} \quad (6.b)$$

In equation (6.a) and (6.b), λ_n^i and λ_n^{i+1} are the Lagrange multipliers for *i*-th and (*i*+1)-th iteration respectively, α is an inner factor and k_n denotes the normal contact stiffness. At the *i*-th iteration, if the penetration depth g is greater than the penetration tolerance g_t, the contact stiffness is increased through the Lagrange multiplier. The iterations continue until g is less than the penetration tolerance.

After introducing the equivalent viscosity in the chosen visco-elastic model, a static analysis was performed. A generalised visco-elastic Maxwell model was used in the FE analysis, having introduced the Prony series of the relaxation modulus $E(t)$ in equation (7.a), then modified with the equivalent approach in equation (7.b).

$$E(t) = E_{inf} + \sum_i^r E_i e^{-\frac{t}{\tau_i}} \quad (7.a)$$

$$E_{eq}(t) = E_{inf,eq} + \sum_i^r E_i e^{-\frac{t}{C(x)\cdot\tau_i}} \quad (7.b)$$

In the equations (7) E_{inf} is the modulus at infinite time, for which successive variations are negligible, τ_i is the relaxation time equal to η_i/E_i (with η_i and E_i visco and elastic parameters respectively of the generalised Maxwell model) and t is the (reduced) time elapsed from the load application. Finally, $C(x)$ is the correction factor for the equivalent approach, which is written:

$$C(x) = \frac{T_a(x)}{\tau_a} \quad (8)$$

Figure 15 shows the generalized Maxwell model associated with the constitutive law assumed for the asphalt layer.

Knowing the relaxation modulus at infinite time, E_{inf}, the corresponding time, t_{inf}, is found. Consequently, $t_{inf,eq}=t_{inf}C_{max}$ will represent the equivalent infinite time associated to the modified relaxation modulus $E_{eq}(t)$. The equivalent infinite time is then used in the FE analysis to estimate the maximum visco-elastic effects that occur in the asphalt layers. Figure summarises the procedure used to define $t_{inf,eq}$.

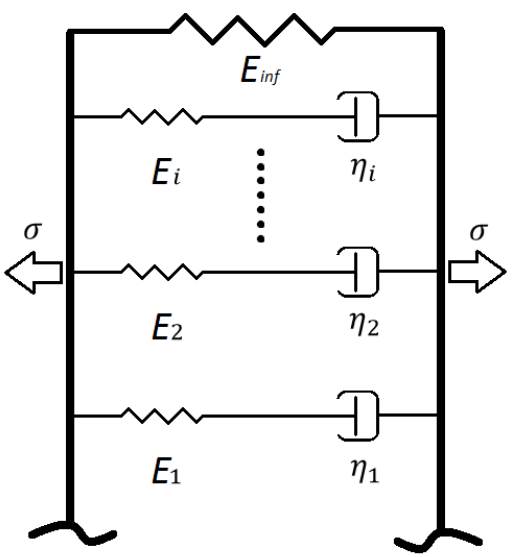

Figure 15 Generalized viscoelastic Maxwell model.

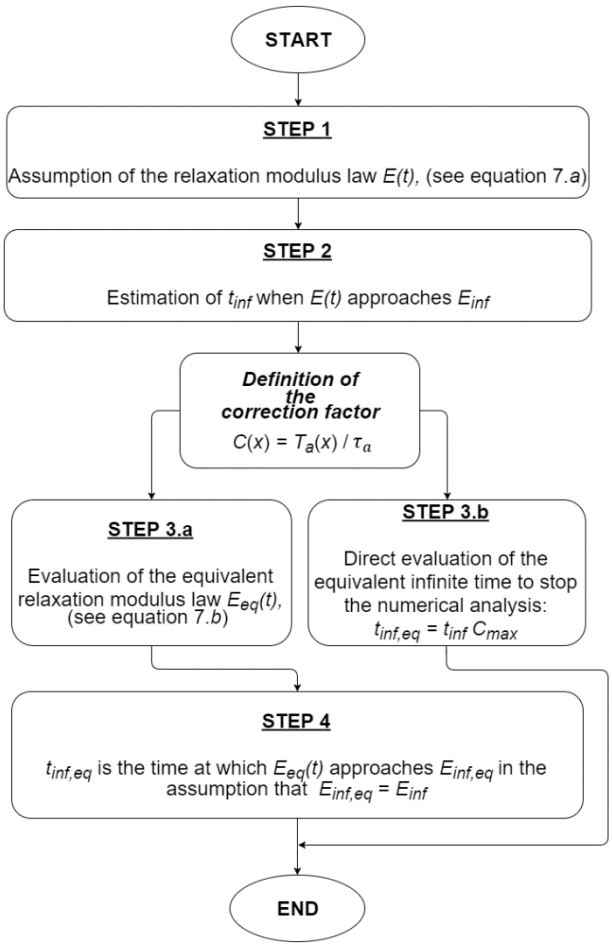

Figure 16 Procedure used to evaluate $t_{inf,eq}$.

Table 3
Prony series parameters at 20 °C (Katicha, 2007).

i	E_i [GPa]	τ_i [s]
1	1.03677	0.9438E-5
2	1.71012	0.9029E-4
3	3.40175	0.7916E-3
4	5.00518	0.5913E-2
5	2.54841	0.6621E-1
6	2.68676	0.4325
7	1.11477	0.3802E1
8	0.398608	0.3776E2
9	0.100638	0.6194E3
10	0.0391743	0.7762E4
11	0.0316236	0.7714E5
12	0.0198995	0.8104E6
E_{inf} = 0.0881144 [GPa]		

Thus, the equivalent viscosity approach was employed to evaluate the long-term visco-elastic deformation of the e-road solution. Simulations were performed in accordance with experimental data taken from literature. In particular, the generalized visco-elastic Maxwell model has been calibrated to material tests reported by Katicha (2007). Table 3 summarises the 12 Prony's terms used for the chain, which demonstrated to be sufficient to fit the experimental data. As for loads, the following input data were used:

- $a_s = 2$ (numbers of axles of a normal vehicle);
- $a_w = 3$ (numbers of axles of a heavy vehicle);
- τ_a= 0.015 s (vehicle speed 70 km/h)

About the load intensity q, the parameters of the bimodal Gaussian distribution (Chengming et al., 2011) were assumed to be:

- $\mu_s = 12{,}705\ N$;
- $\sigma_s = 1{,}407\ N$;
- $\mu_w = 134{,}424\ N$;
- $\sigma_w = 2{,}784\ N$;
- p_s and p_w: values from 0 to 1 with 0.1 increment.

Moreover, the peculiarity represented by e-roads in terms of augmented weight of electric vehicles has been taken into account by adding 5,000 N to μ_s.

About the number of vehicles, the parameters of the thinned Poisson process (Chengming et al., 2011) were defined as:

- $\lambda = 0.02385$
- t_f parameter to be estimated from a recursive procedure.

Finally, the parameters for the transverse frequency distributions (same values assumed for both Gaussian and Laplace processes) were set at:

- $\mu_G = 1\ m$;
- $\sigma_G = 0.19799\ m$.

The results of the probabilistic analysis have highlighted the importance of the assumed value for p_w, the probability of passage of a heavy vehicle. As it can be seen from Figure 17.*a* and 17.*b* passing from p_w=0.1 (associated to T_{95w}=418 s), to p_w=0.9 (associated to T_{95w}=47 s) results in a non-uniform increase of the vertical displacements. A comparison between Figure 17.*a* and 17.*b*, shows that the main differences between e-roads and t-roads concerns the central part of the lane, where the presence of the coil-box limits visco-displacements.

When working with e-roads, rather than the absolute values of displacements, it is important to evaluate the *gap* between the e-road surface and the coil-box, in order to draw conclusions regarding possible damage to the charging device, and on vehicle drivability. As regard the

probabilistic analysis, the *gap* remains quite constant with a decrement of T_{95w} (see Figure 17.*a*), reaching negligible values.

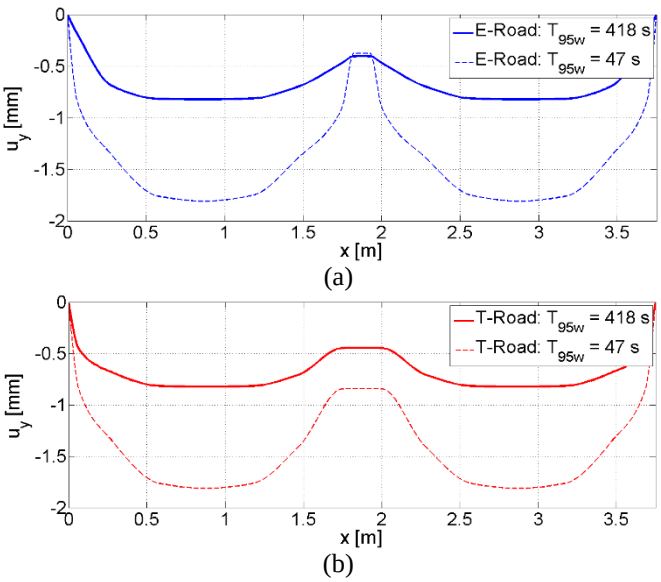

Figure 17 Vertical visco-displacements at infinite time, u_y [mm], of the entire lane (3.75 [m] wide) for e-road (a) (model with contact elements) and t-road (b). $C(x)$ in equation 8 was discretised in 14 different values over x.

Figure 18 reports the same comparison in term of vertical visco-displacements but obtained from HCM design data. In this case, the results show that the maximum *gap* (calculated values after 6.25e6 cycles) reaches approximatively 0.003 m (see also Figure 19). This numerical finding may be critical in e-roads as it can virtually produce vehicle misalignment and additional damage in the charging device. Clearly, the numerical evaluation of the deformations reported in this study constitutes a first outcome that might orient further research on life cycle analysis as well as experimental tests on the recharging technology.

Regarding the deformation of the entire lane (see Figure 18), it is worth specifying that it was obtained by applying the tyre load in different transverse positions x. Important differences are detected again close to the charging device, which transmits the loads to the underlying layers.

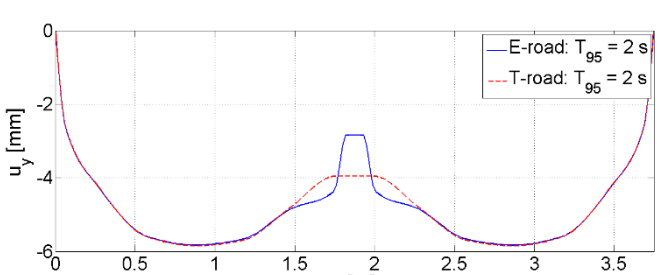

Figure 18 Vertical visco-displacements at infinite time, u_y [mm], of the entire lane (3.75 [m] wide) as obtained from HCM design data.

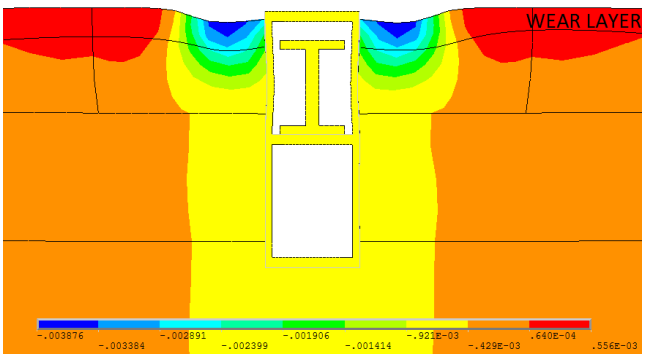

Figure 19 Vertical infinite time visco-displacements u_y [m], at the wheel path (modelled with contact behaviour and design data).

4.2 Fatigue analysis

Tensile horizontal strains and the subsequent distributed cracking are related to the failure of the surface layer of road. Hence, a strain-based approach is used in order to estimate the number of load cycles to failure of the e-road.

To this aim, several analyses have been conducted to evaluate the lifetime of the e-road for different transverse position of the axle (x in Figure 20).

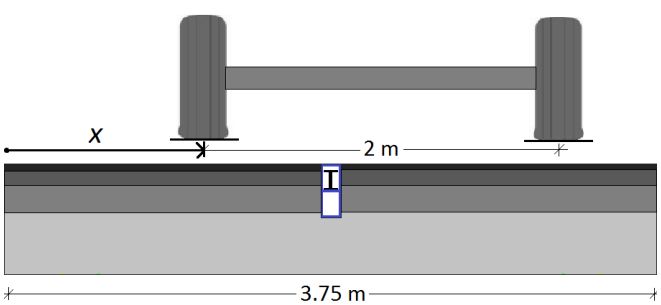

Figure 20 E-road lane with loading axle.

The lifetime of an asphalt layer is commonly defined as the time required for cracks to appear on the pavement section, or for the value of the elastic modulus to reduce to the 50% of its initial value, though this second criterion may be too conservative (Yeo et al., 2008; Huang et al 2014).

Commonly, a general phenomenological law is used to correlate the number of load cycles to failure, N_f, to the value of tensile transverse strain ε at the bottom of the surface layer of pavement (Pais et al., 2009):

$$N_f = k_1 \left(\frac{1}{\varepsilon}\right)^{k_2} \tag{9}$$

As regards equation (9), recent studies have demonstrated a high correlation between the two experimental parameters k_1 (intercept in log-log plane) and k_2 (slope in log-log plane) (Pais et al., 2009; Ren et al., 2012; Zhou et al., 2007). This allows for a reduced number of variables to be determined experimentally.

Parameters k_1 and k_2 in equation (9) were set to the values obtained in (Yeo et al., 2008) with accelerated pavement testing (APT); k_1=1.29E-6 and k_2=3.02. Unlike classical laboratory tests, the APT simulates the road conditions as closely as possible by considering vehicle 'wandering', which results in a longer life estimation.

A fatigue model composed by two extreme damage modes (slip mode and opening mode) about the failure process is then assumed (Manson et al., 1961; Subramanyan and Mater, 1976). The slip and opening modes are taken into account by two separate laws, D_s and D_o respectively:

$$D_s = \frac{\ln(2N_i - 1)}{\ln(2N_f - 1)}; D_o = \frac{\ln(2N_e - 1) - \ln(2N_f - 1)}{\ln(2N_e - 1) - \ln(2N_i - 1)} \quad (10)$$

where N_e is the number of fatigue limit cycles, N_i the ith number of applied load cycles, and N_f is the number of load cycles to failure. To consider simultaneously the presence in each cycle of both slip and opening modes of damage, the D_{so} curve is defined as $D_{so} = D_s \cdot D_o$ (Ben-Amoz, 2009).

The number of cycles N_i corresponds to the ratio between the equivalent time t_{eq} used for the generalised Maxwell model and the inter-arrival time T_a. The strains calculated by the FE model at different positions and for increasing values of t_{eq} were introduced into equation (9) to calculate N_f. When the value D_{so}=1 is attained in the composition of the equations (10), the number of applied load cycles is supposed to have reached the fatigue cycles to failure $N_{fx}(x)$ for different transverse positions.

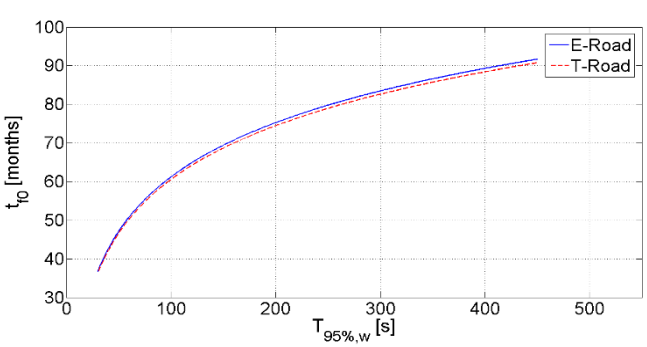

Figure 21 Lifetime of the pavement structure as a function of the inter-arrival time of heavy vehicles.

Anyway, because the lowest number of cycles will control the failure of the structure, the lifetime of the pavement t_{f0} was estimated with N_{f0}=min{$N_{fx}(x)$} as:

$$t_{f0} = N_{f0} \cdot T_a \quad (11)$$

Due to the application of the correction factor, N_{f0}=min{$N_{fx}(x)$} is found when the axle is centred in the road lane. Accordingly, Figure 21 reports the lifetime for both the e-road and the t-road, as a function of the inter-arrival time of heavy vehicles. It can be observed that for low values of T_{95w} (under 150 s) the lifetime decreases rapidly for both e-road and t-road. Moreover, the difference in the lifetime between e-road and t-road decreases with a decrement of T_{95w}, whereas t_{f0} (related to the tensile strain) results to be slightly higher for the e-road than the t-road. The entire computational procedure used to estimate the lifetime of both e-road and t-road pavement is summarised in the flow-chart of Figure 23.

In addition to the probabilistic analysis, an estimation of the lifetime with HCM design data (i.e. q_a= 180 kN, corresponding to a tyre pressure of 1 MPa) has been performed. According to this analysis, t_{f0} reaches values of 184 months and 182 months for the e-road and the t-road respectively.

Figure 22 shows the time evolution of the transverse strains in the e-road, calculated at the bottom of the asphalt layer under the applied load, for both the probabilistic and deterministic (HCM data) case.

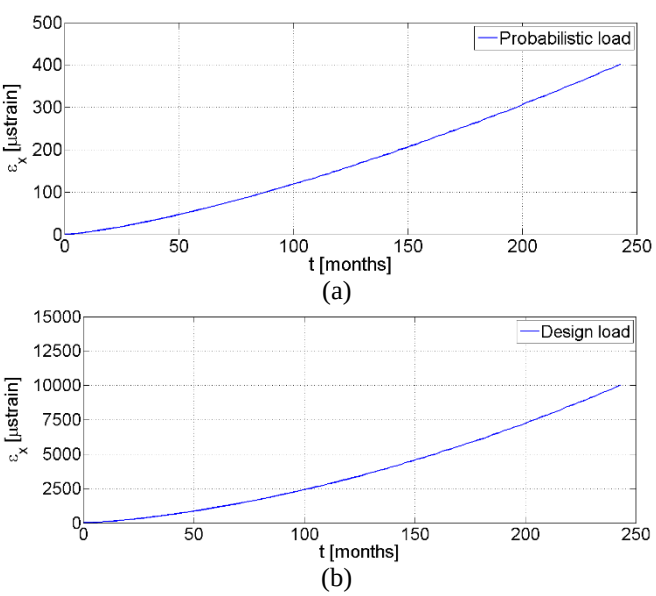

Figure 22 Horizontal transverse strain ε_x [μstrain] evolution at 0.04 m from the road surface, under the applied load in the e-road (model with contact elements) with probabilistic (a) and HCM design (b) loads.

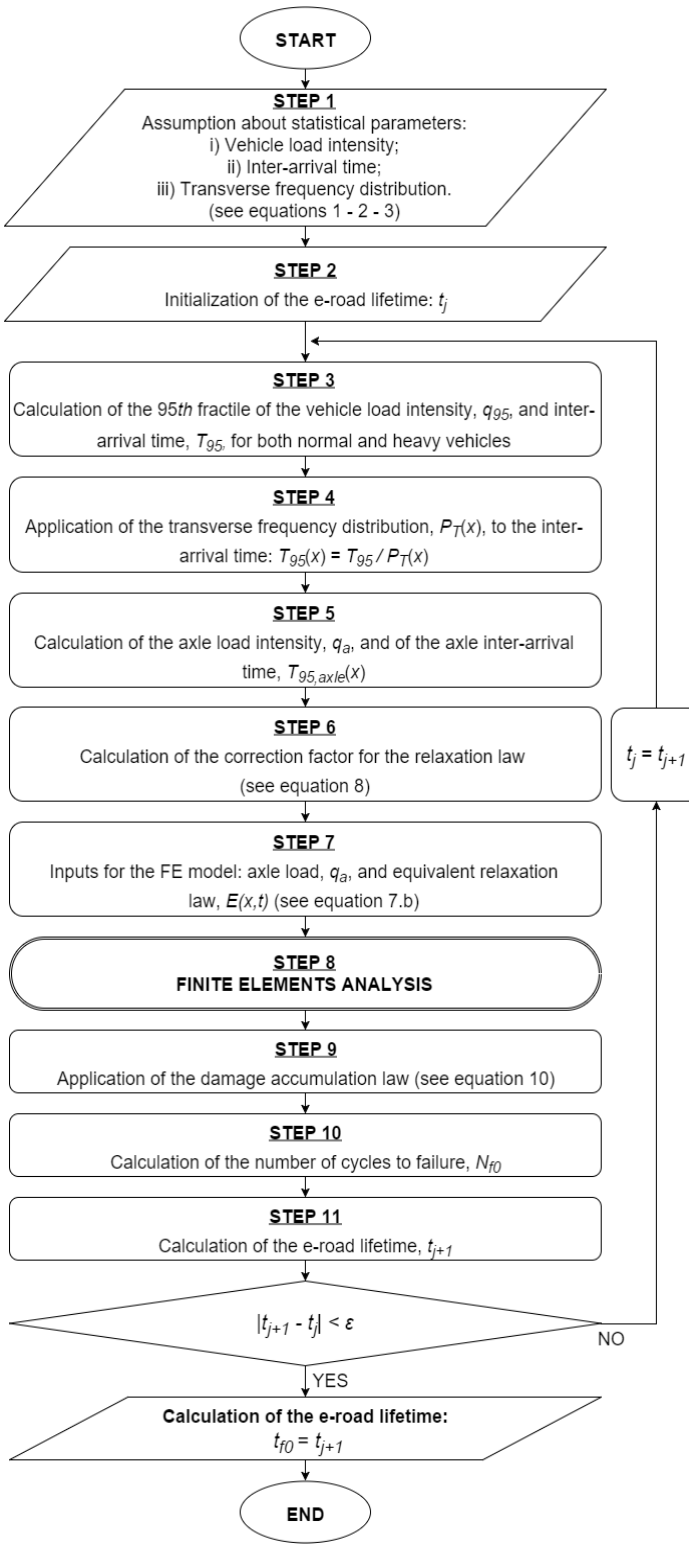

Figure 23 Computational procedure used to evaluate the e-road lifetime, t_{f0}.

5 CONCLUSIONS

This article has presented a new computational methodology for investigating the structural behaviour of e-roads. As an application of such a rationale, the paper reports on the first numerical study on the short- and long-term structural performances of e-road "rail" solutions. Simulations were conducted in order to compare the e-road infrastructure with t-roads, in terms of static, dynamic and fatigue behaviour.

The main results of the numerical study can be summarised as follows:

- In the analysis of the e-roads, models with contact elements allow a more realistic representation of the stress in the pavement. In particular, these models are indispensable for evaluating the long-term visco-elastic deformation, and to estimate the number of cycles at which the e-road starts to show evident degradation.
- The FE viscoelastic analysis, in terms of vertical displacements, has predicted important differential settlements between the e-road surface and the coil-box, amounting to 4-5 millimetres after 660,000 load cycles.
- The visco-elastic analysis has also highlighted critical areas where "strain-storage" typically occurs. Information regarding strain-storage can be helpful in terms of optimizing the position of some non-ferromagnetic sensors for health monitoring purposes.
- Based on fatigue analyses, the e-road (rail solution) had better performance than t-roads, mainly due to the effect of confinement operated by the coil box.

This numerical study presents still some limitations, mainly due to the assumptions about the linear behaviour of the materials. More importantly, results should be integrated with data from active monitoring systems, including sensors embedded in the pavement, even if experimental data from e-road monitoring systems are not available to date.

Future investigations focus on differential settlements of the coil-box, which may potentially affect vehicle drivability and charging device operation. Further research may also concern the effects of temperature and other parameters that are associated with nonlinear behaviour and material degradation. Finally, special attention should be devoted also to possible amplifications caused the introduction of inductive charging technologies at critical points (bridges, viaducts, tunnels etc.).

ACKNOWLEDGMENTS

This research has ε been supported by the European Commission within the FP7 projects UNPLUGGED (Grant N. 314126), and FABRIC (Grant N. 605405).

REFERENCES

Adeli, H., & Cheng, N., (1994), Augmented Lagrangian Genetic Algorithm for Structural Optimization, Journal of Aerospace Engineering, 7(1), 104–118. doi:10.1061/(ASCE)0893-1321(1994)7:1(104)

Agostinacchio, M., Ciampa, D., & Olita, S., (2013), The vibrations induced by surface irregularities in road pavements - a Matlab approach, European Transport Research Review, 1–9. doi:10.1007/s12544-013-0127-8

Ahmed, A., & Erlingsson, S., (2013), Evaluation of permanent deformation models for unbound granular materials using accelerated pavement tests, Road Materials and Pavement Design, 14, 178–195.

Al-Khateeb, L. A., Saoud, A., & Al-Msouti, M. F., (2010), Rutting Prediction of Flexible Pavements using Finite Element Modeling, Jordan Journal of Civil Engineering, 5(2).

Baburamani, P., (1999), Asphalt fatigue life prediction models - A literature review.

Ben-Amoz M., (2009), Cumulative damage model based on two-mode fatigue damage bounds. Materials Science and Engineering, A 504,114–123.

Beskou, N. D., & Theodorakopoulos, D. D., (2011), Dynamic effects of moving loads on road pavements: A review, Soil Dynamics and Earthquake Engineering, 31(4), 547–567. doi:10.1016/j.soildyn.2010.11.002

Blab, R., & Litzka, J., (1995), Measurements of the Lateral Distribution of Heavy Vehicles and its Effects on the Design of Road Pavements, In *Proceedings of the International Symposium on Heavy Vehicle Weights and Dimensions, Road Transport Technology, University of Michigan* (pp. 389–395).

Boys, J. T., & Covic, G. A., (2013a), Basic Concepts, IPT Fact Sheet Series: No. 1.

Boys, J. T., & Covic, G. A., (2013b), Magnetic Circuits for Powering Electric Vehicles, IPT Fact Sheet Series: No. 2.

Chen, F., Taylor, N., & Kringos, N., (2015), Electrification of roads: Opportunities and challenges, Applied Energy, 150, 109–119. doi:10.1016/j.apenergy.2015.03.067

Chengming Lan , Hui Li & Jinping Ou (2011) Traffic load modelling based on structural health monitoring data, Structure and Infrastructure Engineering, 7:5, 379-386, DOI: 10.1080/15732470902726809

Covic, G. A., & Boys, J. T., (2013), Modern Trends in Inductive Power Transfer for Transportation Applications, IEEE Journal of Emerging and Selected Topics in Power Electronics, 1(1), 28–41. doi:10.1109/JESTPE.2013.2264473

Čygas, D., Laurinavičius, A., Paliukaitė, M., Motiejūnas, A., Žiliūtė, L., & Vaitkus, A., (2015), Monitoring the Mechanical and Structural Behavior of the Pavement Structure Using Electronic Sensors, Computer-Aided Civil and Infrastructure Engineering, 30(4), 317–328. doi:10.1111/mice.12104

D'Elia, B., Lanzo, G., & Pagliaroli, A., (2003), Small-Strain Stiffness and Damping of Soils in a Direct Simple Shear Device, In *Pacific Conference on Earthquake Engineering*.

Darabi, M. K., Abu Al-Rub, R. K., Masad, E. A., Huang, C.-W., & Little, D. N., (2012), A modified viscoplastic model to predict the permanent deformation of asphaltic materials under cyclic-compression loading at high temperatures, International Journal of Plasticity, 35, 100–134. doi:10.1016/j.ijplas.2012.03.001

Fisher, T. M., Farley, K. B., Gao, Y., Bai, H., & Tse, Z. T. H., (2014), Electric vehicle wireless charging technology: a state-of-the-art review of magnetic coupling systems, Wireless Power Transfer, 1(02), 87–96. doi:10.1017/wpt.2014.8

Frangopol, D. M., & Messervey, T. B., (2009), Maintenance Principles for Civil Structures, In *Encyclopedia of Structural Health Monitoring*, John Wiley & Sons, Ltd, Chichester, UK. doi:10.1002/9780470061626.shm108

Fraser, M., Elgamal, A., Conte, J. P., Masri, S., Fountain, T., Gupta, A., … El Zarki, M., (2003), Elements of an integrated health-monitoring framework, In T. Kundu (Ed.), (pp. 231–242). doi:10.1117/12.484444

Gill, J. S., Bhavsar, P., Chowdhury, M., Johnson, J., Taiber, J., & Fries, R., (2014), Infrastructure Cost Issues Related to Inductively Coupled Power Transfer for Electric Vehicles, Procedia Computer Science, 32, 545–552. doi:10.1016/j.procs.2014.05.459

Guena, T., & Leblanc, P., (2006), How Depth of Discharge Affects the Cycle Life of Lithium-Metal-Polymer Batteries, In *INTELEC 06 - Twenty-Eighth International Telecommunications Energy Conference* (pp. 1–8), IEEE. doi:10.1109/INTLEC.2006.251641

Gupta, A., Kumar, P., & Rastogi, R., (2014), Critical review of flexible pavement performance models, KSCE Journal of Civil Engineering, 18(1), 142–148. doi:10.1007/s12205-014-0255-2

Harris, D. K., (2007), Lateral load distribution and deck design recommendations for the sandwich plate system (SPS) in bridge applications, Virginia Polytechnic Institute and State University.

Huang, J., Liuand, W., and Sun, X. (2014), "A Pavement Crack Detection Method combining 2D with 3D information based on Dempster-Shafer Theory," Computer-Aided Civil and Infrastructure Engineering, 29:4, pp. 299-313.

ICNIRP, (1998), Guidelines for limiting exposure to time-varying electric, magnetic, and electromagnetic fields (up to 300 GHz). International Commission on Non-Ionizing Radiation Protection., Health Phys, 74(4), 494–522. Retrieved from http://view.ncbi.nlm.nih.gov/pubmed/9525427

ICNIRP, (2010), Guidelines for limiting exposure to time-varying electric and magnetic fields (1 Hz to 100 kHz), Health Physics, 99(6), 818–836.

Jeong, J.-H., Park, J.-Y., Lim, J.-S., & Kim, S.-H., (2014), Testing and modelling of friction characteristics between concrete slab and subbase layers, Road Materials and Pavement Design, 15(1), 114–130. doi:10.1080/14680629.2013.863161

Ju, S.-H., (2009), Finite element investigation of traffic induced vibrations, Journal of Sound and Vibration, 321(3-5), 837–853. doi:10.1016/j.jsv.2008.10.031

Katicha S.,W., (2007), Analysis of Hot-Mix Asphalt (HMA) Linear Viscoelastic and Bimodular Properties Using Uniaxial Compression and Indirect Tension (IDT) Tests. Virginia Polytechnic Institute and State University, Blacksburg, Virginia.

Kettil, P., Lenhof, B., Runesson, K., & Wiberg, N.-E., (2007), Simulation of inelastic deformation in road structures due to cyclic mechanical and thermal loads, Computers & Structures, 85(1-2), 59–70. doi:10.1016/j.compstruc.2006.08.060

Lak, M. A., Degrande, G., & Lombaert, G., (2011), The effect of road unevenness on the dynamic vehicle response and ground-borne vibrations due to road traffic, Soil Dynamics and Earthquake Engineering, 31(10), 1357–1377. doi:10.1016/j.soildyn.2011.04.009

Levenberg, E., (2013), Analysis of pavement response to subsurface deformations, Computers and Geotechnics, 50, 79–88. doi:10.1016/j.compgeo.2012.12.011

Manson S.,S., Nachtingall A.J., Freche J.C., (1961), Proc. ASTM 61, 679–703.

Metrisin J.T., (2008), Guidelines for obtained contact convergence. International ANSYS conference.

Miner, M.,A., (1945), Cumulative damage in fatigue, Journal of Applied Mechanics, 12(3), 159–164.

Mun S., Chehab G.,R., Kim Y.,R., (2007) Determination of time-domain viscoelastic functions using optimized interconversion techniques. Road Materials and Pavement Design, 8(2): 351-365.

National Research Council, (2000). Highway Capacity Manual - HCM200. Transportation Research Board.

Pais, J. C., Pereira, P. A. A., Minhoto, M. J. C., Fontes, L. P. T. L., Kumar, D., & Silva, B. T. A., (2009), The prediction of fatigue life using the k1-k2 relationship, In *2nd Workshop on Four Point Bending* (pp. 39–46).

Park, H., Kim, J., Kim, Y., & Lee, H., (2005), Determination of the layer thickness for long-life asphalt pavements, W: EASTS, 791–802.

Perret, J., & Dumont, A.-G., (2004), Strain and stress distributions in flexible pavements under moving loads, Road Materials and Pavement Design, 5(sup1), 203–225. doi:10.1080/14680629.2004.9689993

Pinotti, E., (2013), Vibration in smart infrastructure systems for electric vehicles, Turin, Italy. Retrieved from http://opac.biblio.polito.it:80/F/?func=direct&doc_number=000360040&local_base=TESW

Qiao, Y., Dawson, A., Huvstig, A., & Korkiala-Tanttu, L., (2015), Calculating rutting of some thin flexible pavements from repeated load triaxial test data, International Journal of Pavement Engineering, 16(6), 467–476. doi:10.1080/10298436.2014.943127

Rahman, M. S., & Erlingsson, S., (2015), Predicting permanent deformation behaviour of unbound granular materials, International Journal of Pavement Engineering, 16(7), 587–601. doi:10.1080/10298436.2014.943209

Ren, X.-W., Tang, Y.-Q., Li, J., & Yang, Q., (2012), A prediction method using grey model for cumulative plastic deformation under cyclic loads, Natural Hazards, 64(1), 441–457. doi:10.1007/s11069-012-0248-8

Rim, C. T., (2013), The development and deployment of on-line electric vehicles (OLEV).

Saevarsdottir, T., & Erlingsson, S., (2015), Modelling of responses and rutting profile of a flexible pavement structure in a heavy vehicle simulator test, Road Materials and Pavement Design, 16(1), 1–18. doi:10.1080/14680629.2014.939698

Sarma, K.C. and Adeli, H., (2002) "Life-Cycle Cost Optimization of Steel Structures", International Journal for Numerical Methods in Engineering, Vol. 55, No. 12, pp. 1451-1462.

Schroeder, A., & Traber, T., (2012), The economics of fast charging infrastructure for electric vehicles, Energy Policy, 43, 136–144. doi:10.1016/j.enpol.2011.12.041

Seo, Y., & Kim, Y. R., (2008), Using Acoustic Emission to monitor fatigue damage and healing in Asphalt Concrete, KSCE Journal of Civil Engineering, 12(4), 237–243. doi:10.1007/s12205-008-0237-3

Subramanyan S., Mater J., (1976), Technol. 98, 316–321.

Suh, I. S., (2011), Application of shaped magnetic field in resonance (SMFIR) technology to future urban transportation, In *CIRP design conference*.

Syabillah S., Pakharuddin M.S., Hishamuddin J., Roslan A.R. and Mohammad S.B., (2012), Groundhook Control of Semi-Active suspension For Heavy Vehicle. International Journal of Research in Engineering and Technology (IJRET) Vol. 1, No. 3, 2012 ISSN 2277 – 4378.

Viktoria Swedish ICT, (2013), Slide-in Electric Road System, Gothenburg, Sweden.

Yeo, I., Suh, Y., & Mun, S., (2008), Development of a remaining fatigue life model for asphalt black base through accelerated pavement testing, Construction and Building Materials, 22(8), 1881–1886. doi:10.1016/j.conbuildmat.2007.04.015

Zhang, J., Andrus, R. D., & Juang, C. H., (2005), Normalized shear modulus and material damping ratio relationships, Journal of Geotechnical and Geoenvironmental Engineering, 131(4), 453–464.

Zhou, F., Hu, S., Scullion, T., Chen, D., Qi, X., & Claros, G., (2007), Development and verification of the overlay tester based fatigue cracking prediction approach, Journal of the Association of Asphalt Pavement Technologists, 76, 627–662.

Zopf, C., Garcia, M. A., & Kaliske, M., (2015), A continuum mechanical approach to model asphalt, International Journal of Pavement

Engineering, 16(2), 105–124. doi:10.1080/10298436.2014.927065

2016-04-05

A computational methodology for assessing the time-dependent structural performance of electric road infrastructures

Ceravolo, Rosario

Wiley

Rosario Ceravolo, Gaetano Miraglia, Cecilia Surace and Luca Zanotti Fragonara. A computational methodology for assessing the time-dependent structural performance of electric road infrastructures. Computer-Aided Civil and Infrastructure Engineering, Volume 31, Issue 9, þÿ S e p t e m b e r 2 0 1 6 , p p 7 0 1 7 1 6

http://dx.doi.org/10.1111/mice.12199